# Effect of Repetitive Processing on the Mechanical Properties and Fracture Toughness of Dynamically Vulcanized iPP/EPDM Blends

**Wei-Kang Wang, Wei Yang, Rui-Ying Bao, Bang-Hu Xie, Ming-Bo Yang**

*College of Polymer Science and Engineering, Sichuan University, State Key Laboratory of Polymer Materials Engineering, Chengdu, 610065 Sichuan, China*

**ABSTRACT:** The effect of repetitive processing on the mechanical properties and fracture toughness of dynamically vulcanized isotactic polypropylene/ethylene-propylene-diene rubber blends (TPVs) with and without addition of β-nucleating agent (β-NA) was studied. The results showed that the repetitive processing did not cause much loss in the mechanical properties of TPVs, especially for TPVs with β-NA, and TPVs with β-NA showed better performance stability than TPVs without β-NA. Essential work of fracture (EWF) approach was used to study the fracture behavior, and the results showed that the value of $w_e$ (the specific essential work of fracture) of TPVs without β-NA showed a significant decrease while that of TPVs with β-NA almost kept constant after repetitive processing. Differential scanning calorimetry and wide-angle X-ray diffraction were used to study the variation of crystalline structures, and the results indicated that the repetitive processing showed no significant influence on the crystalline structures of TPVs, and the β-NA maintained high-nucleating efficiency after repetitive processing. © 2010 Wiley Periodicals, Inc. J Appl Polym Sci 120: 86–94, 2011

**Key words:** repetitive processing; dynamically vulcanized iPP/EPDM blends (TPVs); β-phase; mechanical properties; fracture toughness

## INTRODUCTION

Polypropylene (PP) is a general purpose resin with extensive usage and promising market prospect, but its low-temperature brittleness restricts its application. Various rubbers such as ethylene–propylene–diene rubber (EPDM) were blended with isotactic polypropylene (iPP) to improve its impact toughness. The materials prepared by blending a thermoplastic with an elastomer, such as iPP/EPDM blends, are usually called thermoplastic elastomers (TPE).[1–8] As TPE combines the elastic properties of rubbers and melt processability of thermoplastics, it grows so fast in the field of polymer blends.[2,9] TPEs have lots of important applications including cable and wire, especially in mineral, electronic equipment, constructions, and automotives industries.

In recent years, TPEs based on EPDM and iPP have a remarkable increase in popularity.[1,10] The blends of cross-linked EPDM and PP can be prepared in a roll mill or extruder by the "dynamic vulcanization" method in which EPDM is vulcanized under shear with curing agent at elevated temperature, and the resultant materials, thermoplastic vulcanizates (TPVs),

have been widely used in plastic industry.[11–15] Compared with unvulcanized EPDM/PP blends, the properties, such as the oil resistance, permanent set, ultimate mechanical properties, fatigue resistance, heat deformation, melt strength among others, of EPDM/PP-based TPVs are improved.[6] The enhanced properties of TPVs are attributed to the unique morphology that small and uniform cross-linked rubber particles finely distribute in the PP matrix.

rThe waste plastic materials cause critical problems in environment, which bring about more and more attention from the public. Traditional methods used to solve the problems include incineration, landfill, and so on. However, recycling and utilization of waste plastics might be more beneficial.[16–19] For example, Phuong et al.[20] studied the influence of the recycling processing of homopolypropylene on the mechanical, thermal, and rheological properties. Ismail and Suryadiansyah[21] studied the effect of degradation on the tensile properties of PP/natural rubber (NR) and PP/recycle rubber (RR) blends and found that at a similar rubber content and degradation condition, PP/RR blends exhibited a higher percentage of retention of tensile strength and Young's modulus than PP/NR blends. Thermogravimetric analysis shows that the thermal stability of PP/RR blends is higher than that of PP/NR blends. Jacob et al.[22] replaced raw EPDM (R-EPDM) rubber in PP/EPDM blends with waste ground EPDM (W-EPDM) vulcanizate and found that

although a drop in mechanical properties of the blends was observed at lower loadings of W-EPDM, the properties showed improvement at intermediate W-EPDM loadings. In addition, the R-EPDM/W-EPDM/PP blends were found to be reprocessable.

To evaluate the recyclability and the effect of recycling on the performance variation of polymer materials, repetitive processing method was commonly used. Dintcheva et al.[23] and Camacho and Karlsson[24] have evaluated the properties of recycled PP, PE, and their blends by repeat extrusions. Jansson et al.,[17] Boldizar et al.,[25] and Luzuriaga et al.[26] investigated aging and repeated processing behaviors of used PP, PE, and so on. Tian et al.[27] found that the mechanical properties of the TPVs based on EPDM/PP blends almost remained the original state after repeated processing by backmixing on a two-roll mill at the temperature of 180°C with processing time ranging in 0–60 min.

In our previous work, we introduced β-nucleating agent (β-NA) into TPVs based on iPP/EPDM blends and found that the β-phase of PP dramatically enhanced the fracture toughness of TPVs.[28] In this work, the effect of repetitive processing on the mechanical properties and fracture toughness of dynamically vulcanized iPP/EPDM blends with and without β-NA was studied.

## EXPERIMENTAL PART

### Material

The following materials were used in this study. β-NA used was WBG-II, a powder composed of rare-earth organic compounds, which was purchased from Guangdong Weilinna Functional Material Company, P. R. China. iPP, with the trademark T30s, a resin with a melt flow rate of 2.3 g/10 min (ASTM D1238, 230°C, and 2.16 kg load) was purchased from Lanzhou Petrochemical Company, P. R. China. EPDM (Nordel 4725p) obtained from Dupont Dow Elastomers L.L.C., Wilmington, DE, has these properties: (a) contains 70% ethylene and 4.9% ENB (ethylidene norbornene); (b) Mooney viscosity ($ML_{2+10}^{125°C}$) 25; (c) $\overline{M}_w$ 135,000 g/mol. Phenolic resin (PF) was obtained from Yuantai Biochemistry industry Company, P. R. China, with the trade mark TXL-201, and its properties are softening point at 75°C to 95°C, the content of methylol 6.0653747.5%, the content of water ≤1.0%, and the content of bromine ≤4.0%.

### Sample preparation

The samples were divided into two groups, denoted as G1 and G2, respectively. The two group of samples were of the same compositions except that G2 contains 0.5 wt % (to the weight of the blends) β-NA. The content of vulcanization agent, phenolic resin (PF), was 2 wt %.

The melt reactive blending process for preparing TPV samples (PP : EDPM = 50 : 50 wt %) of the two groups was carried out in an SHJ-20 corotating twin-screw extruder with a screw diameter of 25 mm, a length/diameter ratio of 23, and a temperature profile of 175°C, 185°C, 190°C, and 185°C from the feeding zone to the die. PP, EPDM, and phenolic resin with or without β-NA were simply mixed first and then added into the twin-screw extruder. The extrudate was then pelletized. After drying to remove the attached moisture during extrusion, a certain amount of the pellets was put aside as the first sample of G1 or G2. The remains were extruded again. Using this procedure, five times repetitive processing was conducted and five samples for G1 and G2 groups were prepared, referred to as G1-1, G1-2, G1-3, G1-4, and G1-5 for G1 group and G2-1, G2-2, G2-3, G2-4, and G2-5 for G2 group, respectively. For example, G2-3 refers to the sample of G2 experienced thrice extrusion. All the pellets of the 10 samples were dried and injection molded on a PS40E5ASE precise injection-molding machine (Nissan, Japan), with a temperature profile of 180°C, 200°C, 220°C, and 215°C from the feeding zone to the nozzle. Both the injection pressure and the holding pressure were 30 MPa. The obtained samples were heat pressed for 10 min in a compression mold machine (XLB-D 400 × 400 × 2) into 0.5-mm-thick sheets, with a temperature of 200°C and a pressure of 10 MPa. The compression-molded sheets were then cooled to room temperature under pressure.

### Tests

#### Differential scanning calorimetry (DSC)

The materials taken from the compression molded samples were studied by means of a TA Q20 differential scanning calorimeter. The samples were heated up to 200°C at a rate of 10°C/min under a nitrogen atmosphere and held at 200°C for 5 min to eliminate the influence of thermal history. Afterward, the samples were cooled to 40°C at a rate of 10°C/min and then heated again to 200°C at a heating rate of 10°C/min, with samples of about 5 mg. The melting curve of the second run was recorded.

#### Wide-angle X-ray diffraction (WAXD)

WAXD measurements were carried out with a DX-1000 X-Ray diffractometer at room temperature. The Cu K-alpha (wave length = 0.154056 nm) irradiation source was operated at 50 kV and 30 mA. Patterns were recorded by monitoring diffractions from 5° to 50°, and the scanning speed was 3°/min.

#### Morphology observation

The phase morphology was characterized with a JEOL JSM-5900LV scanning electron microscope

(SEM). The samples were frozen in liquid nitrogen for 30 min and were then cryogenically fractured in liquid nitrogen for SEM analysis. The freshly fractured surface was gold sputtered before SEM analysis. The accelerate voltage was 20 kV. The SEM photographs were also used to analyze the particle size and particle size distribution using a computer image analyzer. The number of particles for each sample was between 300 and 600.

Gel content

The gel contents of the samples were determined by extraction of 0.3 g of powdered sample through a 120-mesh stainless steel pouch in boiling cyclohexane in accordance with ASTMD-2765.

Mechanical properties

The tensile test was performed on an AGS-J universal material test machine (Shimadzu Instrument, Japan) according to ASTM D638-82a. The crosshead speed was 50 mm/min. The flexural test was performed on an AGS-J universal material test machine (Shimadzu Instrument, Japan) according to ASTM D-790. At least five samples were used for each measurement, and the average results were reported.

Fracture toughness

The rectangular (length × width = 100 × 35 mm) double-edged notch tension (DENT) specimens (ligament length: 2–14 mm) were cut from the compression-molded sheets. Deep blunt notches were induced on both sides of the specimens by a sharp knife. The cut notches were sharpened by a fresh razor blade to produce the sharp precrack that was required. Initial notches were made perpendicularly to the tensile direction with a fresh razor blade, obtaining at least 17 specimens for each set. The lengths and thicknesses of the ligament were measured before the test using a reading microscope and a Vernier caliper.

Static tensile tests on the DENT specimens were performed on an Instron universal testing machine (model 5567) test machine at 25°C, and the crosshead speed was 5 mm/min. The load versus displacement curves were recorded, and the absorbed energy until failure was calculated by computer integration of loading curves.

## RESULTS AND DISCUSSION

### Crystalline structures and morphologies

Crystalline structures

Figure 1 gives the heating scan of TPVs samples from G1 and G2 groups. It can be seen that heating
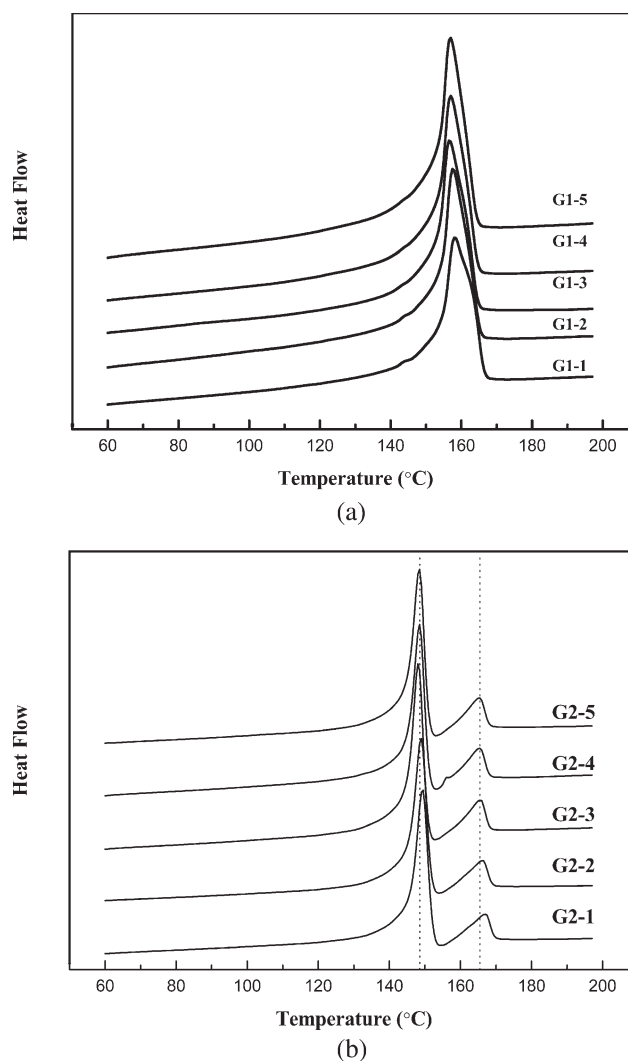
**Figure 1** Effect of repetitive processing on the DSC heating scan of TPVs samples: (a) G1 group and (b) G2 group.

curves of G1 show only endothermic peak of α-phase appeared at 157°C. For the melting behavior of the samples of G2, two endothermic peaks appear at 148°C and 165°C, corresponding to the melting peaks of β-iPP and α-iPP, respectively.[29–32] The melting peak temperature, melting enthalpy, and the half-peak width for samples of both groups are almost the same, indicating that the crystalline structure of the TPVs are not affected by the repetitive processing up to five times.

The WAXD patterns of TPVs samples of G1 and G2 are shown in Figure 2. For samples of G1 group, the reflections at $2\theta = 13.9°$, $16.7°$, $18.4°$, $21.0°$, and $21.7°$ correspond to the (110), (040), (130), (131), and (041) reflections of α-iPP, respectively. For samples of G2 group, two main reflections are clearly observed at $2\theta = 16.0°$ and $21.0°$, which are the characteristic reflections of the (300) and (301) planes of β-iPP, respectively. At the same time, the transformation of α-form to β-form owing to the addition of
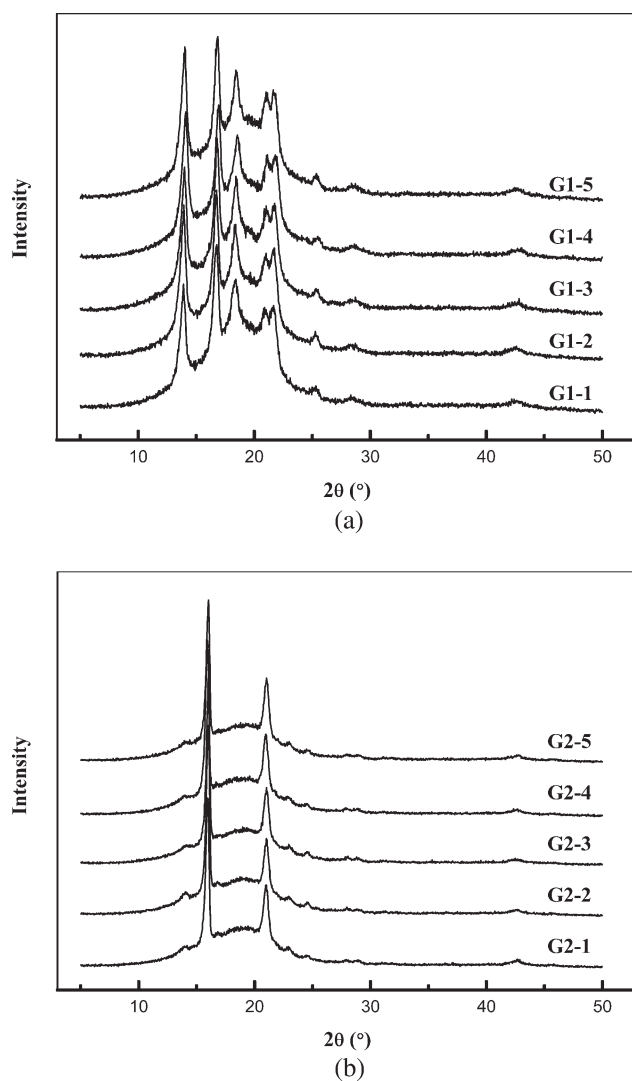
**Figure 2** Effect of repetitive processing on the WAXD profiles of TPVs samples: (a) G1 group and (b) G2 group.

β-NA substantially weakened the diffraction peaks of α-form.[29–32] The relative β crystalline content ($K_\beta$) can be calculated according to the equation suggested by Turner-Jones et al.[33]

$$K_\beta = \frac{H_{300}^\beta}{H_{110}^\alpha + H_{040}^\alpha + H_{130}^\alpha + H_{300}^\beta} \quad (1)$$

where $H_{110}^\alpha$, $H_{040}^\alpha$, $H_{130}^\alpha$ are the intensity of the (110), (040), and (130) reflections of α phase, and $H_{300}^\beta$ is the intensity of (300) reflection of β phase. Here, all the diffraction data were corrected for background (air and instrument) scattering before analysis.

Effect of repetitive processing on total crystallinity of TPVs, β-crystallinity and the $K_\beta$ value of G2 are shown in Table I. The relative β-phase content of all the samples of G2 maintained above 97%. It is evident that β-NA maintains high-nucleating efficiency and thermal stability after repetitive processing.[34,35]

With processing cycles increasing, the total crystallinity of TPVs from G1 group increases slightly whereas the total crystallinity of TPVs from G2 group fluctuates between 55.92% and 60.64% whereas the β-crystallinity almost keeps constant. These results further verify that the repetitive processing shows little influence on the crystalline structures of TPVs with and without β-NA.

Morphologies

Figures 3 and 4 give the morphology of the TPVs of G1-1, G1-5 and G2-1, G2-5. It can be seen that all the samples exhibit a typical two-phase morphology consisting of rubber particles dispersed in the PP matrix.

The weight average diameter $d_w$ of rubber particles can be determined as[36,37]

$$d_w = \sum_i n_i d_i^2 / n_i d_i \quad (2)$$

Assuming the particle size distribution of dispersed phase fits log-normal distribution, the frequency $f(d_i)$ of a particle size $d_i$ is[38]

$$f(d_i) = \frac{1}{\sqrt{2\pi}\ln\sigma} \exp\left[\frac{-(\ln d_i - \ln d)^2}{2\ln^2\sigma}\right] \quad (3)$$

where $d$ and σ, the particle size distribution, are given by[38]

$$\ln d = \frac{\sum\limits_{i=1}^{N} n_i \ln d_i}{\sum\limits_{i=1}^{N} n_i} \quad (4)$$

$$\ln \sigma = \sqrt{\frac{\sum\limits_{i=1}^{N} n_i (\ln d_i - \ln d)^2}{\sum\limits_{i=1}^{N} n_i}} \quad (5)$$

in the case of monodispersity, σ = 1; and for polydispersity, σ > 1.

Table II shows the weight average diameter $d_w$ and particle size distribution, σ of TPVs from G1 and G2 groups and the morphology evolution owing to repetitive processing can be analyzed quantitatively. The particle size of TPVs from G2 group decreased gradually in the repetitive process; from an overall perspective, the particle size of TPVs from G1 group also decreased, although less prominent. Particle size distribution of TPVs from both G1 and G2 groups increased first and then decreased, yet still broader than original level. The development of
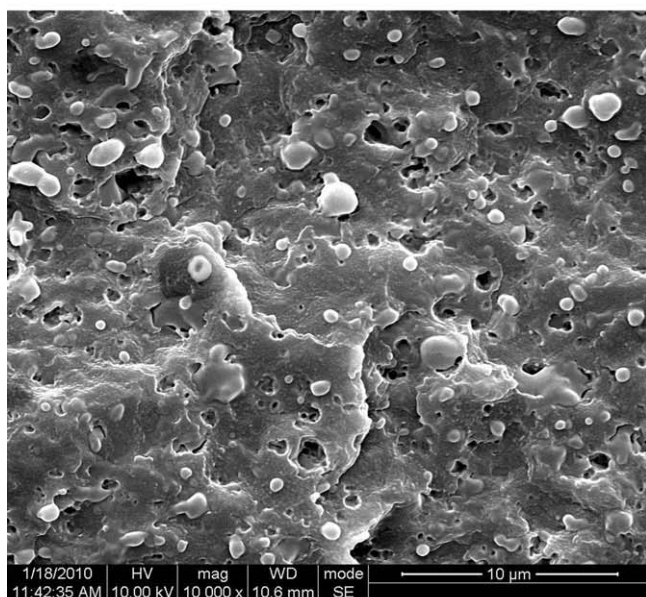
**TABLE I**
**Total Crystallinity of TPVs, β-Crystallinity and the $K_\beta$ Value of G2 with Different Processing Cycles**

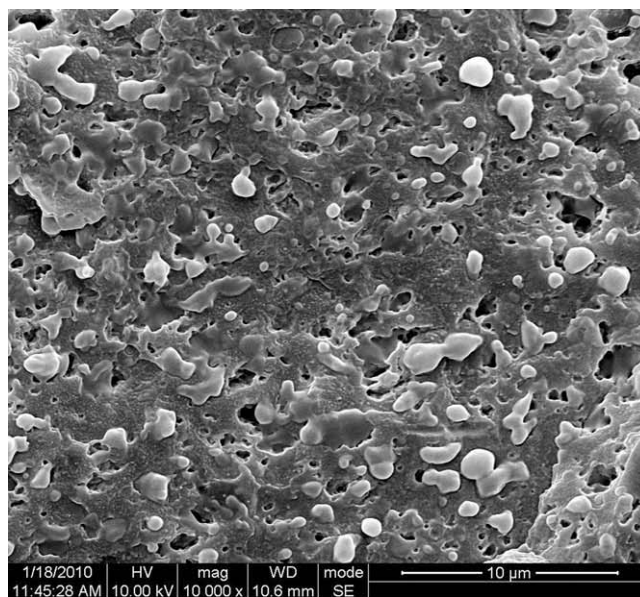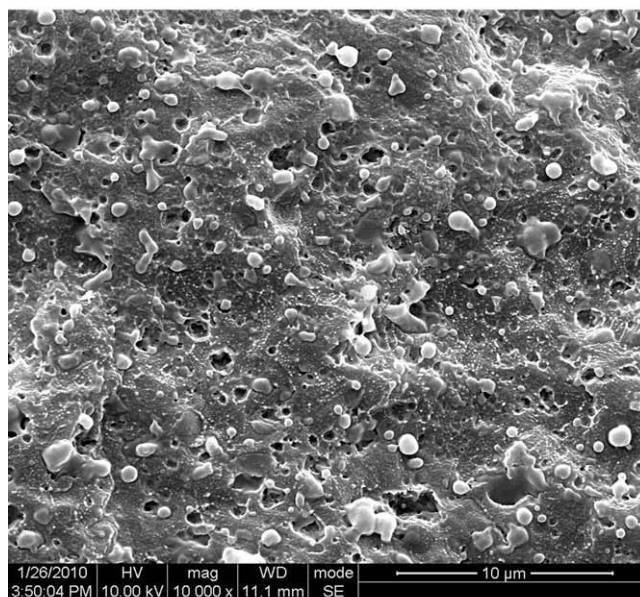| Processing cycle | G1 Total crystallinity (%) | G2 Total crystallinity (%) | β-crystallinity (%) | $K_\beta$ |
|---|---|---|---|---|
| 1 | 36.26 | 55.92 | 47.24 | 97.29 |
| 2 | 39.16 | 56.20 | 47.04 | 97.30 |
| 3 | 40.33 | 59.66 | 49.25 | 97.75 |
| 4 | 41.64 | 60.64 | 49.04 | 97.90 |
| 5 | 43.42 | 58.77 | 48.58 | 97.54 |
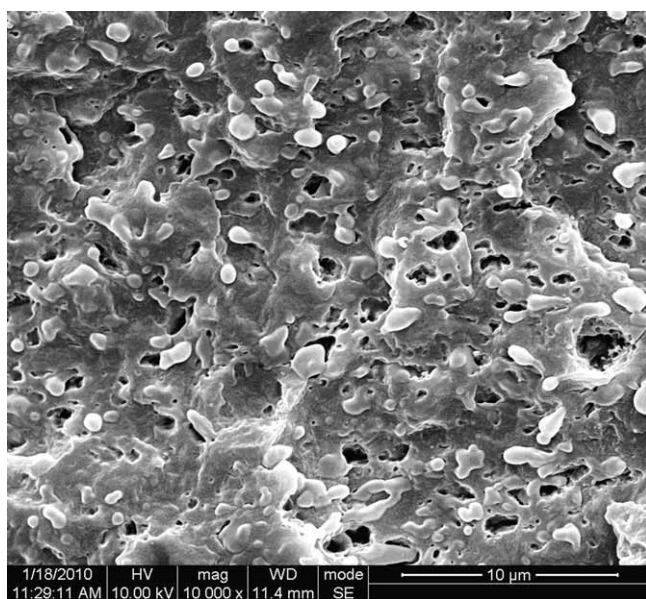


(a)



(b)

**Figure 3** SEM micrographs of the samples from G1: (a) G1-1 and (b) G1-5.

(a)



(b)

**Figure 4** SEM micrographs of the samples from G2: (a) G2-1 and (b) G2-5.

**TABLE II**
**Weight Average Diameter $d_w$ and Particle Size Distribution σ of Rubber Particles for TPVs with Different Processing Cycles**

| Processing cycle | G1 $d_w$ (µm) | σ | G2 $d_w$ (µm) | σ |
|---|---|---|---|---|
| 1 | 0.81 | 1.30 | 0.82 | 1.41 |
| 2 | 0.88 | 1.43 | 0.80 | 1.44 |
| 3 | 0.67 | 1.55 | 0.75 | 1.47 |
| 4 | 0.74 | 1.49 | 0.66 | 1.45 |
| 5 | 0.74 | 1.46 | 0.64 | 1.42 |

Gel Content, Tensile Properties, and Flexural Properties of TPVs with Different Processing Cycles

| Processing cycle | G1 | | | | | G2 | | | | |
|---|---|---|---|---|---|---|---|---|---|---|
| | $GC^a$ | $E^b$ | $\sigma_y^c$ | $E_f^d$ | $\sigma_t^e$ | $GC^a$ | $E^b$ | $\sigma_y^c$ | $E_f^d$ | $\sigma_t^e$ |
| 1 | 4.6 | 366 | 10.1 | 225 | 8.54 | 4.5 | 212 | 10.2 | 158 | 8.05 |
| 2 | 5.0 | 335 | 11.2 | 201 | 8.47 | 4.8 | 196 | 10.2 | 143 | 8.05 |
| 3 | 4.2 | 311 | 10.4 | 196 | 8.30 | 3.8 | 204 | 9.76 | 145 | 8.06 |
| 4 | 4.3 | 309 | 10.9 | 190 | 8.22 | 3.7 | 203 | 9.54 | 147 | 8.06 |
| 5 | 4.3 | 266 | 10.9 | 188 | 8.20 | 3.5 | 193 | 9.49 | 154 | 8.05 |

[a] Gel content (%).
[b] Tensile modulus (MPa).
[c] Tensile yield strength (MPa).
[d] Flexural modulus (MPa).
[e] Flexural strength (MPa).

the morphology can be described as a dynamic process controlled by the rate of breakup and the coalescence of the rubber droplets as two mutual mechanisms.[39]

## Gel content and mechanical properties

The gel content and mechanical parameters of samples from G1 and G2 groups are listed in Table III. With the processing cycle increasing, the maximum gel content occurs at the second cycle, possibly due to the incomplete cross-linking reaction in the first cycle, and the processing of the second cycle provide a chance to complete the cross-linking reaction. Then, the gel content drops for a certain degree from the third-processing cycle because the rubber particles break up owing to the high shear in the extrusion, resulting in the breaking down of some cross-linking bond and the decrease of the cross-linking density.[27] However, the gel content remains almost unchanged after the following reprocessing.

Overall, the tensile and flexural strength and modulus of samples with β-NA (G2 group) are lower than those of samples without β-NA (G1 group), which is the reasonable result of the presence of large amount of β phase in samples of G2 group, owing to the better fracture toughness but lower tensile modulus, yield strength, flexural modulus and flexural strength of β phase compared with α phase.[29–32,40]

With the processing cycle increasing, the tensile modulus and flexural modulus of samples from G1 group show a declining trend; finally, the tensile modulus has fallen from 366 MPa to 266 MPa and the flexural modulus has fallen from 225 MPa to 188MPa. However, both the tensile modulus and flexural modulus of samples from G2 group were almost unchanged with the increase of processing cycle. In addition, the differences in the tensile yield strength and flexural strength of samples from both groups are very small, and with repetitive process-

ing, the variations of tensile strength and flexural strength for both groups, less than about 1 MPa, are also neglectable, especially for the G2 group with β-NA.

Although scission of macromolecular chains and oxidative degradation are unavoidable, but the increasing total crystallinity, the morphology evolution, the enhanced interfacial interaction, and the stable relative content of β phase crystals can make up for the loss in mechanical properties of TPVs, especially those with β-NA (G2 group). Therefore, the repetitive processing does not cause great loss in the mechanical properties of both groups, especially for G2 group, and the TPVs with β-NA show more stable performance than those without β-NA.

## Fracture toughness

Recently, the essential work of fracture (EWF) method has gained great attention and popularity for the facture behavior description of ductile polymers, toughened polymer blends and composites, especially for fracture tests of sheets and films because of experimental simplicity.[41–59] The important correlations can be written as follows:

$$W_f = W_e + W_p \tag{6}$$

$$W_e = w_e BL \tag{7}$$

$$W_p = w_p \beta BL^2 \tag{8}$$

$$w_f = W_f/BL = w_e + \beta w_p L \tag{9}$$

where $L$ is the ligament length, $B$ is the specimen thickness, and β is a shape factor associated with the plastic zone. The total energy $W_f$ required to fracture a precracked specimen can be partitioned into the essential work of fracture, $W_e$, which is proportional to the ligament area (LB) and the nonessential or plastic work of fracture, $W_p$, which is proportional to the volume of the yield zone ($BL^2$). $w_f$, $w_e$, and $w_p$ stand for the specific total work of fracture, the
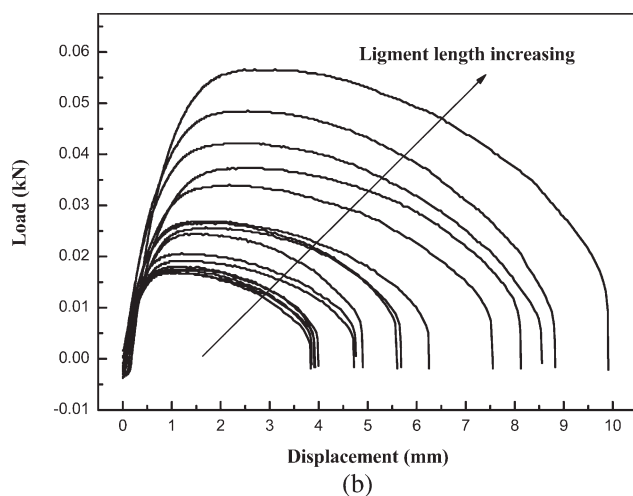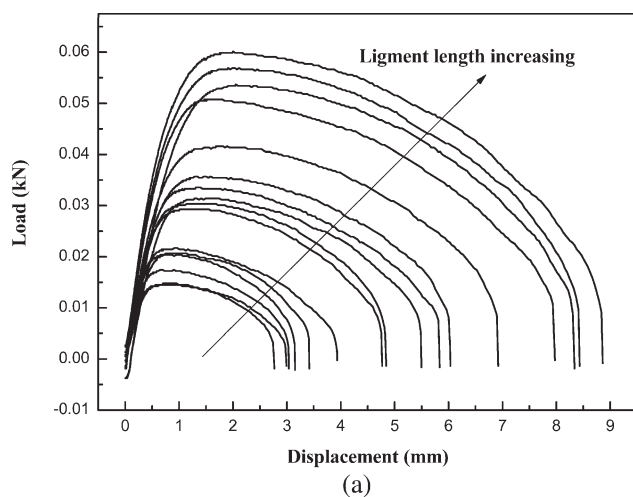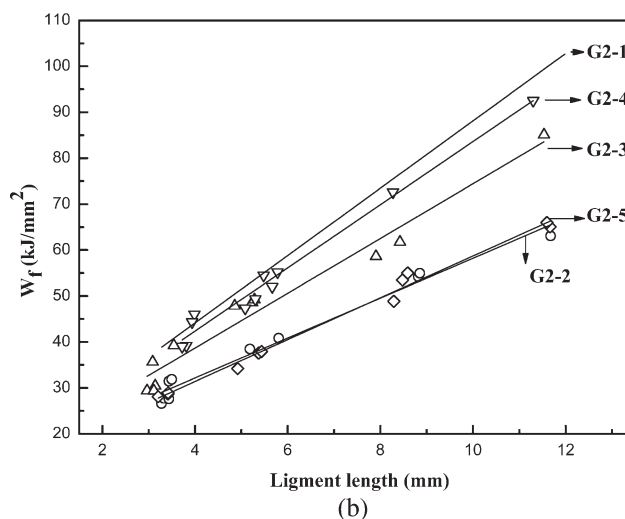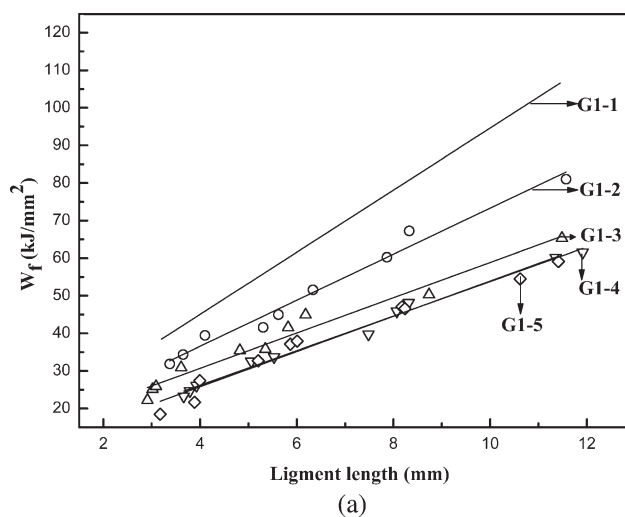
**Figure 5** Typical plots of load versus displacement of TPVs from both groups: (a) G1-3 and (b) G2-5.



**Figure 6** Specific work of fracture against ligament length for (a) samples of G1 group and (b) samples of G2 group.

specific essential work of fracture, and the specific nonessential work of fracture, respectively. The value of $w_e$ is a material constant, only dependent on the thickness of the specimen; it can be used to characterize the fracture toughness and has been demonstrated theoretically to be equivalent to $J_{IC}$. By extrapolating the curve of $w_f$ versus $L$ to zero ligament length, the value of $w_e$ can be obtained from the intercept and the value of $\beta w_P$ can be obtained from the slope of the regression lines as suggested by eq. (9).

The load-displacement curves of DENT specimens of G1-3 and G2-5 are shown in Figure 5, on behalf of other samples of the two groups. In these curves, the load increased quickly with a slight increase of the displacement before the upper point in the initial stage. After the peak, a smooth and slow drop in load occurred with further increase of displacement and suddenly a rapid load drop at the end stage of the curves signaling the fracture of the specimens.

A precondition for EWF method is that the ligament length is fully yielded before crack growth. According to the load-displacement curves in Figure 5, no full ligament yielding occurs before crack growth, whereas yielding occurs simultaneously with crack growth, which makes the using of the EWF approach tolerable when all other prerequisite of the EWF are met.[30] At the same time, the curves were obtained for DENT specimens with different

**TABLE IV**
**Fracture Parameters for the TPVs Based on PP/EPDM Blends Without β-NA Nucleating Agent (G1 Group)**

| Sample | $w_e$ (kJ/m$^2$) | $\beta w_P$ (MJ/m$^3$) | $R^2$ |
|--------|------------------|------------------------|-------|
| 1–1    | 12.0             | 8.3                    | 0.92  |
| 1–2    | 12.1             | 6.1                    | 0.96  |
| 1–3    | 12.0             | 4.7                    | 0.93  |
| 1–4    | 7.8              | 4.6                    | 0.98  |
| 1–5    | 7.1              | 4.7                    | 0.93  |

**TABLE V**
**Fracture Parameters for the TPVs Based on PP/EPDM Blends with β-NA Nucleating Agent (G2 Group)**

| Sample | $w_e$ (kJ/m$^2$) | $\beta w_p$ (MJ/m$^3$) | $R^2$ |
|---|---|---|---|
| 2–1 | 14.9 | 7.3 | 0.97 |
| 2–2 | 14.8 | 4.3 | 0.96 |
| 2–3 | 14.8 | 6.0 | 0.92 |
| 2–4 | 14.9 | 6.9 | 0.96 |
| 2–5 | 13.2 | 5.0 | 0.98 |

ligament length; good self-similarity of the curves was shown in each group. The maximum load, the displacement to failure, and the area under the curves all increased regularly with increasing ligament length, indicating that the mode of fracture is independent of ligament length and the cracks propagate under similar stress condition. This is another important criterion of EWF approach, so the EWF measurements are valid at this deformation rate for the TPVs prepared.[47,48,53]

The plots of $w_f$ versus $L$ of samples of G1 and G2 groups are shown in Figure 6. It is worthwhile noting that the diagrams gave very good linear relationships for all the TPVs studied, as proved by the linear regression coefficient ($R^2$), being in most cases higher than 0.95. The values of $w_e$ and $\beta w_p$ are also listed in Tables IV and V.

From Table IV, it is obvious that the $w_e$ for G1 declines with the increase of processing cycle; particularly after the fourth cycle, the value of $w_e$ is reduced by about 40%. $\beta w_p$ is also dropped by more than 40% after the third cycle, indicating less plastic energy absorbed with further increase in the processing cycle.

From Table V, it can be seen that all the values of $w_e$ for samples of G2 group are higher than that of G1 group because of the presence of β-phase that improves the fracture toughness of TPVs obviously.[3,7] Compared with G1-1, the value of $w_e$ for G2-1 has granted an increase of about 25%. More significant is that the value of $w_e$ for samples of G2 group keep stable though it decreases slightly after the fifth processing cycle. This result indicates that the β-NA not only enhances the toughness of TPVs due to the induced β-phase but also maintains its high efficiency after repetitive processing. For samples of G2 group, there is no significant change in the value of $\beta w_p$, which just fluctuates between 4.3 and 7.3 MJ/m$^3$. Different from the case in pure PP, the β-phase shows stronger effect on the crack growth than on the plastic deformation owing to the introduction of EPDM. Hence, no significant changes for the energy for plastic deformation absorbed during the fracture process.[28] From what has been discussed earlier, we may safely draw a conclusion that the introduction of β-NA into TPVs-based EPDM/

PP can effectively preserve toughness of TPVs after repetitive processing.

**CONCLUSIONS**

The effect of repetitive processing on the mechanical properties, fracture toughness, crystalline structures, and morphologies of dynamically vulcanized iPP/EPDM blends was studied, and the following conclusions were drawn:

1. The repetitive processing does not alter the crystalline structures and crystallinity of TPVs based on dynamically vulcanized iPP/EPDM blends with and without β-NA, and the β-NA used maintains high-nucleating efficiency after repetitive processing.
2. The repetitive processing does not cause much loss to mechanical properties of the TPVs with and without β-NA, especially for those with β-NA and the TPVs with β-NA show more stable performance than those without β-NA.
3. The β-NA induced β-phase indeed enhance the fracture toughness of the TPVs and with the processing cycle increasing, the value of $w_e$ of TPVs without β-NA showed a significant drop whereas the value of $w_e$ of TPVs with β-NA almost kept constant.

**References**

1. Paul, D. R.; Newman, S. Polymer Blends; Academic Press: New York, 1978.
2. Legge, N. R.; Holden, G.; Schroeder, H. E.; Thermoplastic Elastomer: A Comprehensive Review; Hanser: Munich, 1987.
3. Varga, J.; Garzó, G.; Makromol Chem 1990, 180, 15.
4. Coran, A. Y.; Patel, R. P. In Thermoplastic Elastomers, 2nd ed.; Holden, G., Ed.; Hanser: New York, 1996; p VII/153 ff.
5. Coran, A. Y. In Handbook of Elastomers: New Developments and Technology; Bhowmick, A. K.; Stephens, H. L., Eds.; Marcel Dekker: New York, 2001; p 265.
6. Yu, L.; Wang, W.; Xiao, W. Polym Degrad Stab 2004, 86, 69.
7. Grein, C.; Plummer, C. J. G.; Kausch, H.-H.; Germain, Y.; Béguelin, Ph. Polymer 2002, 43, 3279.
8. Grein, C.; Gahleitner, M.; Polym Lett 2008, 2, 392.
9. De, S. K.; Bhowmick, A. K. Thermoplastic Elastomers From Rubber Plastic Blends; Horwood: London, 1990.
10. Yamaguchi, M.; Miyata, H.; Niua, K. J Appl Polym Sci 1996, 62, 87.
11. US 3,758,643 (1973), invs.: W. K. Fisher.
12. US 3,862,106 (1975), invs.: W. K. Fisher.
13. Coran, A. Y.; Patel, R. Rubber Chem Technol 1981, 54, 892.
14. Coran, A. Y.; Patel, R. Chem Technol 1983, 56, 210.

15. Coettler, L. A.; Richwine, J. R.; Wille, F. J. Rubber Chem Technol 1982, 55, 1448.
16. Santos, A. S. F.; Agnelli, J. A. M.; Trevisan, D. W.; Manrich, S. Polym Degrad Stab 2002, 77, 441.
17. Jansson, A.; Möller, K.; Gevert, T. Polym Degrad Stab 2003, 82, 37.
18. Wallis, M.; Bhatia, S. K. Polym Degrad Stab 2006, 91, 1476.
19. Miskolczi, N.; Bartha, L.; Deak, G. Polym Degrad Stab 2006, 91, 517.
20. Phuong, N. T.; Gilbert, V. J Reinf Plast Compos 2008, 27, 1983.
21. Ismail, H.; Suryadiansyah, Polym Plast Technol 2004, 43, 319.
22. Jacob C.; De P. P.; Bhowmick, A. K.; De, S. K. J Appl Polym Sci 2001, 82, 3304.
23. Dintcheva, T. N.; La Mantia, F. P.; Acierno, D.; Di Maio, L.; Camino, G.; Trotta, F. Polym Degrad Stab 2001, 72, 141.
24. Camacho, W.; Karlsson, S. Polym Degrad Stab 2002, 78, 385.
25. Boldizar, A.; Jansson, A.; Gevert, T.; Möller, K. Polym Degrad Stab 2000, 68, 317.
26. Luzuriaga, S.; Kovárová, J.; Fortelny, I. Polym Degrad Stab 2006, 91, 1226.
27. Tian, H. C.; Wu, S. M.; Han, J. B.; Feng, Y. X.; Zhang, L. Q. China Synthetic Rubber Industry 2004, 27, 34.
28. Tang, X. G.; Bao, R. Y.; Yang, W.; Xie, B. H.; Yang, M. B.; Hou, M. Eur Polym J 2009, 45, 1448.
29. Karger-Kocsis, J.; Varga, J. J Appl Polym Sci 1996, 62, 291.
30. Karger-Kocsis, J.; Varga, J.; Ehrenstein, G. W. J Appl Polym Sci 1997, 64, 2057.
31. Karger-Kocsis, J. Plast Rubber Compos Process Appl 1997, 26, 372.
32. Karger-Kocsis, J.; Varga, J.; Ehrenstein, G. W. J Appl Polym Sci 1999, 73, 1205.
33. Turner-Jones, A. Aizlewood, J. M.; Beckelt, D. R. Makromol Chem 1964, 75, 134.
34. Xiao, W. C.; Wu, P. Y.; Feng, J. C. J Appl Polym Sci 2008, 108, 3370.
35. Qin, Y. W.; Feng, J. C.; Guo, S. H.; Zheng, D.; Huang, R.; Qian, Y. Y. New Chem Mater 2007, 35, 56.
36. Jiang, W.; Liu, C. H.; Wang, Z. G.; An, L. J.; Liang, H. J. Jiang, B. Z.; Wang, X. H.; Zhang, H. X. Polymer 1998, 39, 3285.
37. Borggreve, R. J. M.; Gaymans, R. J.; Schuijer, J.; Housz, J. I. Polymer 1987, 28, 1489.
38. Irani, R. R.; Callis, F. C. Particle Size: Measurement, Interpretation and Application; Wiley: New York, 1963.
39. Goharpey, F.; Katbab, A. A.; Nazockdast, H. J Appl Polym Sci 2001, 81, 2531.
40. Chen, H. B.; Karger-Kocsis, J.; Wu, J. S.; Varga, J. Polymer 2002, 43, 6505.
41. Broberg, K. B. Int J Fract 1968, 4, 11.
42. Mai, Y.-W.; Cotterell, B. Int J Fract 1986, 32, 105.
43. Mai, Y.-M.; Cotterell, B.; Horlyck, R.; Vigna, G. Polym Eng Sci 1987, 27, 804.
44. Mai, Y.-W.; Powell, P. J Polym Sci Part B 1991, 29, 785.
45. Wu, J.; Mai, Y.-W.; Cotterell, B. J Mater Sci 1993, 28, 3373.
46. Wu, J.; Mai, Y.-W. Polym Eng Sci 1996, 36, 2275.
47. Karger-Kocsis, J. Polym Bull 1996, 37, 119.
48. Karger-Kocsis, J. J Polym Eng Sci 1996, 36, 203.
49. Karger-Kocsis, J.; Czigany, T. Polymer 1996, 37, 2433.
50. Karger-Kocsis, J.; Czigany, T.; Moskala, E. J. Polymer 1997, 38, 4587.
51. Karger-Kocsis, J.; Czigany, T.; Moskala, E. J. Polymer 1998, 39, 3939.
52. Mouzakis, D. E.; Stricker, F.; Karger-Kocsis, J. J Mater Sci 1998, 33, 2551.
53. Mouzakis, D. E.; Gahleitner, M.; Karger-Kocsis, J. J Appl Polym Sci 1998, 70, 873.
54. Arencon, D.; Velasco, J. I. J Mater Sci 2001, 36, 179.
55. Arkhireyeva, A.; Hashemi, S. Eng Fract Mech 2004, 71, 789.
56. Yang, W.; Shi, W.; Xie, B. H.; Niu, Y. H.; Zuo, M.; Li, Z. M.; Yang, M. B. J Mater Sci 2005, 40, 5323.
57. Gong, G.; Xie, B. H.; Yang, W.; Li, Z. M.; Zhang, W. Q.; Yang, M. B. Polym Test 2005, 24, 417.
58. Gong, G.; Xie, B. H.; Yang, W.; Li, Z. M.; Lai, S. M.; Yang, M. B. Polym Test 2006, 25, 98.
59. Yang, W.; Xie, B. H.; Shi, W.; Li, Z. M.; Liu, Z. Y.; Chen, J.; Yang, M. B. J Appl Polym Sci 2006, 99, 1781.